1-1-2004

Parameterization and Validation of a Lumped Parameter Diffusion Model for Fuel Cell Stack Membrane Humidity Estimation#

Denise McKay
University of Michigan, Ann Arbor, dmckahn@smith.edu

Anna Stefanopoulou
University of Michigan, Ann Arbor

Parameterization and Validation of a Lumped Parameter Diffusion Model for Fuel Cell Stack Membrane Humidity Estimation#

Denise McKay* Anna Stefanopoulou
Fuel Cell Control Laboratory, University of Michigan, Ann Arbor MI

***Abstract*— We present here a model for estimating the electrode humidity of a proton exchange membrane fuel cell (PEMFC) stack. We use this model to develop a nonlinear open loop estimator of the membrane humidity based on monitoring the pressure and temperature entering and exiting the electrodes, as well as the upstream humidity of each electrode. This lumped parameter model, calibrated and experimentally validated, quantifies the average vapor mass transport across a 24 cell, PEMFC stack of 1.4 kW continuous power output. The experimental method devised here for the parameterization of the model is simple and reproducible. The estimator can be used to develop a systematic procedure for warming up and humidifying PEMFC stacks prior to connection of a load.**

I. Introduction

Operating below the boiling point of water, proton exchange membrane fuel cell (PEMFC) stacks utilize the chemical energy from the reaction of hydrogen and oxygen to produce electricity, water and heat. Thus, the fuel delivered to the PEMFC is hydrogen gas and oxygen from the air. As shown in Figure 1, fuel travels through inlet manifolds to the flow fields. From the flow fields, gas diffuses through porous media to the membrane. The membrane, sandwiched in the middle of the cell, typically contains catalyst and microporous diffusion layers along with gaskets as a single integrated unit. One side of the membrane is referred to as the anode, the other the cathode. The anode and cathode are more generally referred to as electrodes. The catalyst layer at the anode separates hydrogen molecules into protons and electrons. The membrane permits ion transfer (hydrogen protons), requiring the electrons to flow through an external circuit before recombining with protons and oxygen at the cathode to form water. This migration of electrons produces useful work.

The ability of the membrane to conduct protons is linearly dependent upon its water content [9]. On one hand, as membrane water content decreases, ionic conductivity decreases ([8], [1], [7]), resulting in a decreased cell electrical efficiency, observed by a decrease in the cell voltage. This decrease in efficiency results in increased heat production which evaporates more water, in turn lowering membrane water content, creating a positive feedback loop resulting in hot spots (membrane damage). On the other hand, excessive water stored in the electrodes obstructs fuel flow, resulting in cell flooding [9]. In both cases, the water concentration in the electrodes is very important for optimal fuel cell efficiency and reliability.

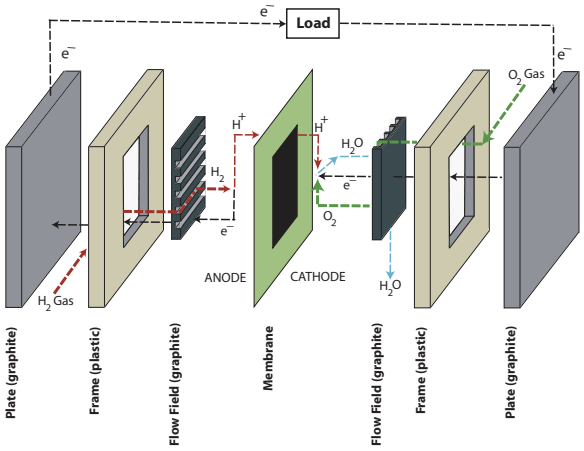

Fig. 1. Fuel cell component description

As with all power systems, the PEMFC system may experience the extremes of hot arid or cold moist environments. These widely varying operating temperatures and humidities greatly impact the control of cell humidification and water removal and are integral to thermal management [4]. Consequently, achieving and maintaining an adequate water balance within the cell under a wide range of operating loads, is critical to successfully optimizing cell performance. Unfortunately, installing humidity sensors in the electrode exit flow is not practical due to vapor condensing on the surface of the sensor. The difficulty of sensing humidity, combined with the importance of this variable motivates an estimator design. To this end, this work develops and validates a lumped parameter model for estimating the relative humidity of the cell electrodes.

We demonstrate that this lumped parameter model can be used to accurately capture the spatially averaged phenomena under certain conditions. The experimental method devised here for the parametrization of the model is simple and reproducible. On the contrary, the existing methods for identifying the vapor mass transport parameters require membrane conditioning and stack disassembly. The proposed method, utilizing measurements of temperature, pressure, flow and relative humidity, quantifies the amount of water entering and exiting each electrode under subsaturated conditions to experimentally determine the vapor

This work is funded by the National Science Foundation under contract CMS-0219623 and CMS-0201332 and the Automotive Research Center (ARC) under U.S. Army contract DAAE07-98-3-0022.

*Corresponding Author, 1082 Walter E. Lay Auto Lab, The University of Michigan, 1231 Beal Avenue, Ann Arbor, MI, 48109, dmckay@umich.edu

transport coefficients used in the model. These coefficients are then used to estimate the electrode relative humidity using practically implementable sensors in a PEMFC stack with 24 cells capable of producing 1.4 kW of continuous power.

II. Nomenclature

The equations presented in this paper use the following symbols and units: m is used for mass (kg), W for mass flow (kg/s), T for temperature (K), P for pressure (Pa) and V for volume (m^3). To denote relative humidity, ϕ is used for the unitless scale from 0-1 and RH is used for 0-100%. The following subscripts are chosen where c is used for cathode, a for anode, e for electrode, v for vapor, dg for dry gas, o for electrode outlet, and i for electrode inlet.

To differentiate theoretical values (x) from modeled, measured, and estimated data, an overbar ($\overline{x}$) represents measurements or calculated variables found using measurements, and a hat ($\hat{x}$) represents estimated variables.

III. Electrode Vapor Mass Balance

The electrical efficiency of a PEMFC depends on the membrane water content that is spatially varying depending on the temperature distribution and the gas humidity at the membrane surface. Due to the complexity inherent with distributed parameter analysis, the geometric complexity of the stack design, as well as the difficulty associated with taking measurements at the membrane surface or within the electrodes of large multi-cell stacks, our effort lumps the electrode RHs by assuming linear gradients from manifold inlet to outlet and across the membrane thickness. Specifically we assume that the average membrane humidity ϕ_m is equal to

$$\phi_m = \frac{\phi_c + \phi_a}{2} \tag{1}$$

where, ϕ_c and ϕ_a are the cathode and anode RH, respectively, that in turn depend on the mass of water stored in the cathode $m_{w,c}$ and anode $m_{w,a}$. Given the temperature dependent electrode (cathode or anode) vapor saturation pressure, $P_{sat,e} = P_{sat}(T_e)$, the electrode relative humidity is $\phi_e = \min\left[1, \frac{m_{w,e} R_v T_e}{p_{sat,e} V_e}\right]$, where, V_e represents the volume of the electrode (m^3), T_e is the temperature of the electrode (K), and R_v is the vapor gas constant (J/kg K).

The rate of change of mass of water $\dot{m}_{w,e}$ stored in the electrodes, shown in Figure 2, is quantified through conservation of mass, accounting for the flow of vapor $W_{v,ei}$ into the electrode, the flow of vapor $W_{v,co}$ exiting the electrode, the flow of vapor $W_{v,m}$ through the membrane from anode to cathode, and the flow of vapor $W_{v,g}$ being generated only in the cathode due to the chemical reduction reaction:

$$\dot{m}_{w,c} = \frac{dm_{w,c}}{dt} = W_{v,ci} - W_{v,co} + W_{v,m} + W_{v,g} \tag{2}$$

$$\dot{m}_{w,a} = \frac{dm_{w,a}}{dt} = W_{v,ai} - W_{v,ao} - W_{v,m}. \tag{3}$$

Note that the rate of change of the mass of water inside the electrodes, $\dot{m}_{w,e}$ depends solely on the summation of vapor flows, because it is assumed that the liquid water does not leave the stack and evaporates into the electrode gas if electrode relative humidity drops below 100%. The mass of water is in vapor form until the RH of the gas exceeds saturation (100%), the point at which vapor condenses into liquid water.

Note also that we assume humidified gas is supplied to the fuel cell, and thus, water enters and exits the cathode and anode as shown in Figure 2. Depending upon the operating conditions and the type of membrane used, the amount of water generated at the cathode from the reduction reaction is typically not substantial enough to maintain the desired level of membrane humidity for significant periods of time. As a result, water vapor is carried to each electrode with the incoming gas streams either external or internal to the stack.

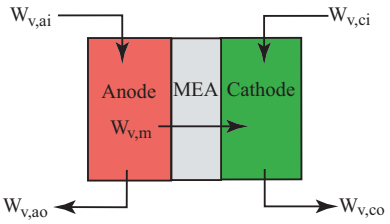

Fig. 2. Schematic of electrode vapor mass balance

The mass flow rate of vapor entering and exiting the electrodes can be calculated using Dalton's Law of Ideal Gases. For simplicity, the equations will be developed generically as a function of the dry gas flow entering and exiting the electrodes which can be measured accurately. For the anode, the dry gas is hydrogen and for the cathode, the dry gas is air. The flow of vapor entering the electrodes is modeled by:

$$W_{v,ei} = \frac{M_v P_{v,ei}}{M_{dg} P_{dg,ei}} W_{dg,ei} = \frac{M_v \phi_{ei} P_{sat,ei}}{M_{dg} P_{dg,ei}} W_{dg,ei}$$

finally,

$$W_{v,ei} = rm_e \frac{\phi_{ei} P_{sat,ei}}{(P_{ei} - \phi_{ei} P_{sat,ei})} W_{dg,ei} \tag{4}$$

where, M_{dg} is the molar mass of the dry gas (kg/mol), M_v is the molar mass of vapor (kg/mol), rm_e is the ratio of molar masses (M_v/M_{dg}), $P_{sat,ei}$ denotes the electrode inlet saturation pressure where $P_{sat,ei} = f(T_{ei})$ (Pa), P_{ei} is the electrode inlet total pressure (Pa), and $W_{dg,ei}$ is the dry gas mass flow entering the electrode (kg/s). The mass flow of dry gas entering the electrodes is determined from measurements of the volumetric flow by accounting for the density of the gas being measured. Similarly, the mass flow rate of vapor exiting the electrode $W_{v,eo}$ is given as

$$W_{v,eo} = rm_e \frac{\phi_{eo} P_{sat,eo}}{(P_{eo} - \phi_{eo} P_{sat,eo})} W_{dg,eo}. \tag{5}$$

The vapor mass generated $W_{v,g}$ is an algebraic relation of the current density i generated at the membrane surface area

A_{fc} as $W_{v,g} = M_v n i A_{fc}/(2F)$ where F is the Faraday number and n the number of cells in the stack.

There are two mechanisms for quantifying the transport of vapor through the membrane $W_{v,m}$, namely, back diffusion and electroosmotic drag. Each ion passing through the membrane carries a constant number of water molecules from the anode to the cathode [5]. This transfer of vapor is known as electroosmotic drag and is a function of the current density (i, A/m^2) produced by the stack. Secondly, the use of humidified gases as well as the production of water at the cathode results in a vapor concentration gradient ($(\phi_c - \phi_a)/t_m$) across the membrane thickness t_m. This concentration gradient causes diffusion of water through the membrane and is referred to as back diffusion. The magnitude and direction of the net vapor flow through the membrane (anode to cathode or cathode to anode) is a function of the relative magnitudes of these two transport mechanisms. The vapor transport across PEM membranes is characterized by the diffusion characteristics D_w using Fick's Law, and the electroosmotic drag coefficient n_d:

$$W_{v,m} = \left[n_d \frac{i}{F} - D_w \frac{\rho_{m,dry}(\phi_c - \phi_a)}{M_{m,dry} t_m} \right] (M_v A_{fc} n) \quad (6)$$

where, $\rho_{m,dry}$ is the membrane dry density, $M_{m,dry}$ is the membrane molar mass.

The model described in Eq. 6 has been applied extensively for modeling water transport in PEMFCs for distributed systems where ϕ_c and ϕ_a are local variables at a point within the electrode ([3], [7], [6]). The distributed nature of diffusion within the flow fields has been researched using a gas chromatograph [2]. However, such measurements are typically completed with small (<50 cm^2) single cells. While useful for addressing material design issues and understanding the complexities of multiphase flow, models based on such measurements have proven to underestimate the quantity of water actually migrating within large multi-cell stacks, especially when considering electroosmotic drag [8].

IV. Parametrization of Vapor Diffusion Across the Membrane

To parameterize the vapor diffusion, we concentrate on the open circuit conditions ($i = 0$). The vapor diffusion is found by substituting (6) into (2) and (3):

$$D_{w,c} = \frac{\mu}{(\phi_c - \phi_a)} \left[W_{v,ci} - W_{v,co} - \frac{dm_{v,c}}{dt} \right] \quad (7)$$

$$D_{w,a} = -\frac{\mu}{(\phi_c - \phi_a)} \left[W_{v,ai} - W_{v,ao} - \frac{dm_{v,a}}{dt} \right] \quad (8)$$

where, $\mu = M_{m,dry} t_m / (\rho_{m,dry} M_v A_{FC} n)$ in m^2/kg is used to simplify Eq. (6). Note that to measure and parameterize the total vapor flow across the membranes, the electrode ϕ_c and ϕ_a must be measured, which requires sub-saturated conditions (RH<100%) at the measurement point. Thus, it is assumed for the parameterization that no liquid water is present at any location within the electrode diffusion layers or flow fields.

If all variables on the right hand side of (7) and (8) are measured or calculated, then these equations provide a redundant means of calculating the vapor diffusion. We utilize this redundancy to check the validity of our assumptions of sub-saturated conditions. If the two values for D_w do not agree, there is additional water storage not accounted for in the model. In this section we first present the location of the measurements taken, and then, using psychrometric and thermodynamic properties, show how measured values are used to experimentally determine a relationship for D_w.

A. Experimental Set-up and Measurements

A 24-cell, 300 cm^2, 1.4kW PEMFC stack containing GORE^{TM} PRIMEA® Series 5620 MEAs[1] was used to experimentally determine the diffusion coefficient. To diffuse gas from the flow fields to the membrane, double-sided, Version 3 ETek^{TM} ELATs were used. The flow fields are machined into graphite plates. The stack utilizes an internal humidification section (GORE^{TM} SELECT® membranes), which diffuses water vapor from the coolant loop to humidify the incoming air.

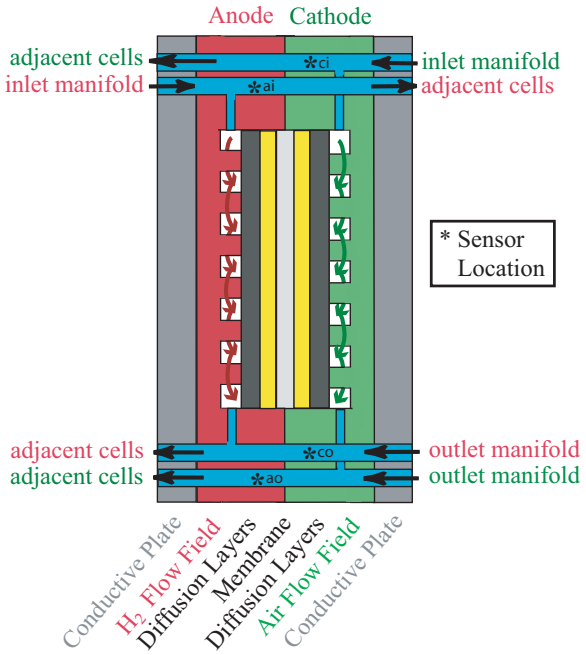

Fig. 3. Locations of sensors

Figure 3 shows a schematic describing the location of the manifolds in relation to the membrane surface. Fuel flows from the inlet manifolds to the active area and then from the active area to the outlet manifolds. Relative humidity measurements were taken in the outlet manifolds of both electrodes and the inlet manifold of the cathode. The anode

[1]The PEMFC stack was purchased from the Schatz Energy Research Center at Humboldt State University

inlet RH (ϕ_{ai}) conditions were measured and found to be constant due to the relatively uniform gas composition of the grade (99.99%) of hydrogen used for testing. Consequently, for all simulations the anode inlet RH was assumed to be constant at 20% RH (ϕ_{ai}= 0.2) at the inlet gas temperature. To maintain sub-saturated conditions at varying air flow rates, the hydrogen flow was held constant using a pressure regulator upstream of the stack and a throttle valve downstream of the stack.

To parameterize the lumped diffusion model we assume temperature, pressure and relative humidity are linearly spatially distributed from the electrode manifold inlets to the outlets. Specifically, the average electrode RH is assumed to be equal to the midpoint electrode RH based on the measured inlet and outlet manifold RH: $\overline{\phi}_e = (\overline{\phi}_{ei}+\overline{\phi}_{eo})/2$, where overbar variables represent the lumped variables that can be measured or calculated directly from measurements.

Figure 4 displays the instrumented stack installed on the test station at the University of Michigan's Fuel Cell Control Laboratory. Protruding from the stack endplates are the relative humidity, temperature and pressure transducers as well as gas and coolant connections. Arrows are used to show the flow of hydrogen and air into and out of the stack.

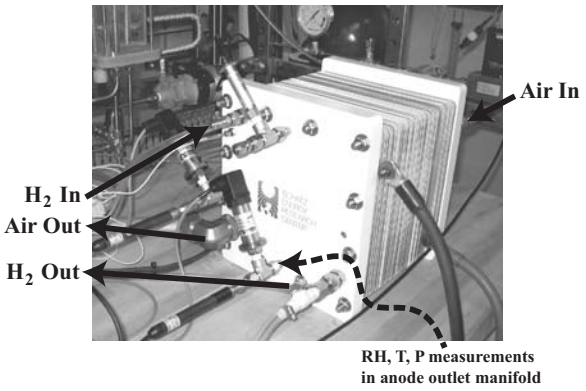

Fig. 4. Instrumented fuel cell stack

Due to physical constraints, the cathode inlet total pressure was not directly measured. Separate experiments were run to determine the functional relationship between the cathode inlet pressure and the incoming dry volumetric airflow rate. For all testing conditions, the dry cathode volumetric inlet airflow was measured upstream of the internal humidification, and the cathode inlet pressure was found using the polynomial function:

$$P_{ci} = \left[0.1245Q_{a,ci}^2 + 15.22Q_{a,ci} + 74.20\right] + 101325$$

where, $Q_{a,ci}$ denotes the volumetric flow of dry air entering the cathode (slm) and P_{ci} represents the cathode inlet total air pressure (Pa).

When the fuel cell stack produces no current ($i = 0$), the gases supplied to the stack are not reacted (as is the case under load). Consequently, the flow of dry gas entering the stack is equal to the flow of dry gas exiting the stack ($W_{dg,eo} = W_{dg,ei}$) and will be denoted by either $\overline{W}_{air}$ for the cathode or $\overline{W}_{H_2}$ for the anode dry gas measurements.

Using the ideal gas law, the time rate of change of the mass of vapor in the electrodes, $\dot{m}_{v,e}$ (kg/s), is described by:

$$\dot{m}_{v,e} = \frac{d}{dt}\left(\frac{P_{v,e}V_e}{R_vT_e}\right) = \frac{V_e}{R_v}\frac{d}{dt}\left(\frac{\phi_e P_{sat,e}}{T_e}\right)$$

which for all our experiments can be approximated as:

$$\overline{\dot{m}}_{v,e} = \frac{V_e\overline{P}_{sat,e}}{R_v\overline{T}_e}\frac{1}{2}\frac{d}{dt}\left(\overline{\phi}_{ei}+\overline{\phi}_{eo}\right). \tag{9}$$

Substituting (4), (5), and (9) into Equations (7) and (8), D_w can be experimentally determined using either the cathode or anode mass balance as shown:

$$\begin{aligned}\overline{D}_{w,c} \;=\; & \frac{\mu}{(\overline{\phi}_c-\overline{\phi}_a)}\left[rm_c\overline{W}_{air}\left(\frac{\overline{\phi}_{ci}\overline{P}_{sat,ci}}{(\overline{P}_{ci}-\overline{\phi}_{ci}\overline{P}_{sat,ci})}-\right.\right.\\ & \left.-\frac{\overline{\phi}_{co}\overline{P}_{sat,co}}{(\overline{P}_{co}-\overline{\phi}_{co}\overline{P}_{sat,co})}\right)-\\ & \left.-\frac{V_c\overline{P}_{sat,c}}{R_v\overline{T}_c}\left(\frac{1}{2}\frac{d}{dt}\left(\overline{\phi}_{ci}+\overline{\phi}_{co}\right)\right)\right]\end{aligned} \tag{10}$$

$$\begin{aligned}\overline{D}_{w,a} \;=\; & -\frac{\mu}{(\overline{\phi}_c-\overline{\phi}_a)}\left[rm_a\overline{W}_{H_2}\left(\frac{\overline{\phi}_{ai}\overline{P}_{sat,ai}}{(\overline{P}_{ai}-\overline{\phi}_{ai}\overline{P}_{sat,ai})}-\right.\right.\\ & \left.-\frac{\overline{\phi}_{ao}\overline{P}_{sat,ao}}{(\overline{P}_{ao}-\overline{\phi}_{ao}\overline{P}_{sat,ao})}\right)-\\ & \left.-\frac{V_a\overline{P}_{sat,a}}{R_v\overline{T}_a}\left(\frac{1}{2}\frac{d}{dt}\left(\overline{\phi}_{ai}+\overline{\phi}_{ao}\right)\right)\right].\end{aligned} \tag{11}$$

B. Diffusion Results

Testing was completed under conditions ranging from 20-80 slm dry airflow, 1-3 slm dry hydrogen flow, 30-60°C manifold temperature, and 1-4 psig hydrogen inlet pressure over the course of 26 separate experimental runs. At each airflow rate, data were analyzed to examine the effect of the dry airflow rate, cell operating temperature, and the electrode inlet and outlet relative humidity on the diffusion coefficients ($\overline{D}_{w,c}$ and $\overline{D}_{w,a}$). Figure 5 displays various measured and calculated data over time for a test conducted at 60 slm dry airflow (approximate airflow required to produce 900 W with an excess ratio of 3). In the first (top most) graph the total vapor mass transport entering and exiting the electrodes ($W_{v,ei}$ and $W_{v,eo}$ from (4) and (5)) are plotted, the second graph displays the calculated value for the total vapor mass transport across the membrane ($\overline{W}_{v,m}$) using both the cathode (10) and anode (11) mass balance, the third graph displays the calculated values for the electrode relative humidity ($\overline{\phi}_c$ and $\overline{\phi}_a$), and the fourth graph includes the electrode inlet and outlet temperatures ($\overline{T}_{ci}$, $\overline{T}_{co}$, $\overline{T}_{ai}$, and $\overline{T}_{ao}$).

At the beginning of the test the thermal management system was shutdown to maintain sub-saturated conditions. As a result, the cathode inlet temperature decreases by 17°C

over the duration of the testing period. This lack of water circulation results in a decreased vapor exchange to the incoming air and thus a lower entering relative humidity. The decrease in cathode RH ($\overline{\phi}_c$) is due to the decrease of cathode inlet RH ($\overline{\phi}_{c,i}$).

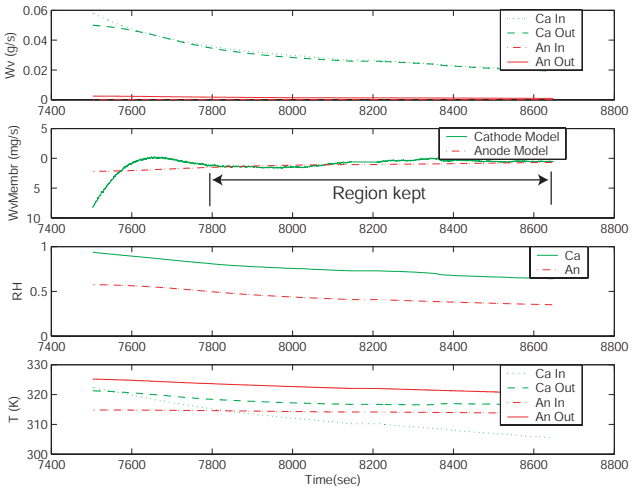

Fig. 5. Test results at 60 slm air flow

As the test progresses, the total vapor mass transport across the membrane ($\overline{W}_{v,m}$), using the anode and cathode mass balance, approach the same values, designated with an arrow. The region where the two models begin to predict similar values confirms the assumptions of 1) an absence of liquid water in the electrodes, 2) sub-saturated conditions throughout the electrode, and 3) linearly spatially distributed RH gradients from inlet to outlet and from cathode to anode, verifying the models capability of estimating the diffusion coefficient. At the beginning of the test, the predictions were not close indicating that additional water was stored in the electrodes (as liquid or vapor) or that RH was not linearly distributed throughout the electrode.

To determine $\overline{D}_{w,c}$ and $\overline{D}_{w,a}$, each data set was analyzed to find a region where the vapor mass transport calculations were confirmed by both the anode and cathode mass balances. We selected the data for which the difference between these diffusion coefficients were within 30%, excluding the data that momentarily predict similar values for $\overline{D}_{w,e}$, as shown in subplot 2 of Figure 5 near the 7500^{th} second.

The diffusion calculated using the anode (11) and cathode (10) mass balance for each experimental data set are then averaged ($\overline{D}_w = (\overline{D}_{w,c} + \overline{D}_{w,a})/2$). The diffusion values for all of the experiments are then plotted versus the membrane RH in the first (top most) graph in Figure 6. The second and third graphs in Figure 6 examine the influence of temperature and the cathode volumetric dry air flow rate on the diffusion coefficient. There is clearly a linear relationship between the membrane relative humidity, temperature and the diffusion coefficient. As the temperature and RH increase, the diffusion coefficient increases. However, the membrane RH is a function of the saturation pressure which is, in turn, a function of the temperature. Thus, RH implicitly accounts for the membrane temperature and a direct relationship between the membrane relative humidity and the diffusion coefficient was made. Least squares regression is used to determine d_{w_1} and d_{w_0} in the following linear approximation of diffusion:

$$D_w = d_{w_1}\phi_m - d_{w_0} \tag{12}$$

Regressing data for all 26 experiments results in dw_1=0.0026 and dw_0=0.00054. Regressing data for one particular experiment gives dw_1=0.0034 and dw_0=0.0000942. When comparing these coefficients, the difference in magnitude results in a difference in the predicted value for the flow of vapor through the membrane and will be further discussed in the next section.

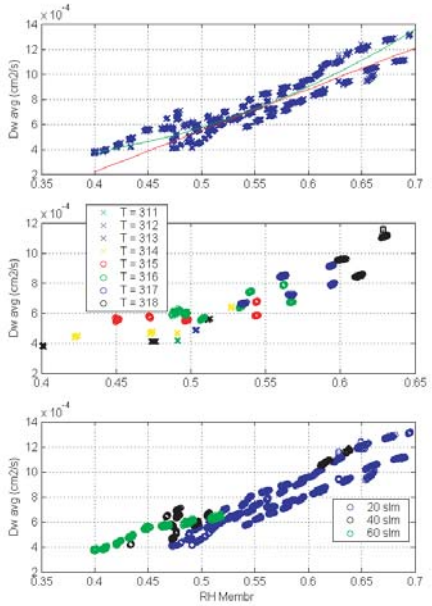

Fig. 6. Diffusion coefficient versus membrane RH

V. Development of Dynamic RH Estimator

The cost of RH sensors and their structural sensitivity to saturated conditions often prohibits their use in real world applications. As a result, the ability to accurately model the RH of the electrodes is desired. Moreover, the model could enhance our understanding of humidity dynamics and the temporal evolution of dehydration and flooding that until now could not be decoupled from temperature or flow conditions. Using the diffusion model in Eq. 12, the time rate of change of the cathode and anode outlet RH can be estimated using (2), together with (4), (5), and (9):

$$\begin{aligned}\frac{d}{dt}\hat{\phi}_{co} &= \frac{2R_v\overline{T}_c}{V_c\overline{P}_{sat,c}}\left[rm_c\overline{W}_{air}\left(\frac{\overline{\phi}_{ci}\overline{P}_{sat,ci}}{\overline{P}_{ci}-\overline{\phi}_{ci}\overline{P}_{sat,ci}}\right.\right.\\ &\left.\left.-\frac{\hat{\phi}_{co}\overline{P}_{sat,co}}{\overline{P}_{co}-\hat{\phi}_{co}\overline{P}_{sat,co}}\right)-\widehat{D}_w\widehat{\Delta\phi}/\mu\right]-\frac{d}{dt}\overline{\phi}_{ci}\end{aligned} \tag{13}$$

$$\frac{d}{dt}\hat{\phi}_{ao} = \frac{2R_v\overline{T}_a}{V_a\overline{P}_{sat,a}}\left[rm_a\overline{W}_{H_2}\left(\frac{\overline{\phi}_{ai}\overline{P}_{sat,ai}}{(\overline{P}_{ai}-\hat{\phi}_{ai}\overline{P}_{sat,ai})}\right.\right.$$
$$\left.\left.-\frac{\hat{\phi}_{ao}\overline{P}_{sat,ao}}{\overline{P}_{ao}-\hat{\phi}_{ao}\overline{P}_{sat,ao}}\right)-\widehat{D}_w\widehat{\Delta\phi}/\mu\right]-\frac{d}{dt}\overline{\phi}_{ai} \quad (14)$$

where $\begin{matrix}\widehat{D}_w \\ \widehat{\Delta\phi}\end{matrix} \begin{matrix}= d_{w_1}\hat{\phi}_m + d_{w_0} \\ = \hat{\phi}_c - \hat{\phi}_a\end{matrix}$ with $\begin{matrix}\hat{\phi}_m \\ \hat{\phi}_c \\ \hat{\phi}_a\end{matrix} \begin{matrix}= (\hat{\phi}_c + \hat{\phi}_a)/2 \\ = (\overline{\phi}_{ci} + \hat{\phi}_{co})/2 \\ = (\overline{\phi}_{ai} + \hat{\phi}_{ao})/2.\end{matrix}$

The resulting second order system is discretized using finite difference approximation and the electrode outlet RH can be estimated. To validate the open loop estimation of the electrode outlet RH, simulations are initialized using the actual measurements of electrode outlet RH. We implement $\frac{d\overline{\phi}_{ci}}{dt}$ from the last two measurements of ϕ_{ci}, similarly for $\frac{d\overline{\phi}_{ai}}{dt}$.

VI. Validation of Open Loop Estimator

As mentioned above, the diffusion coefficient found by satisfying (12) was completed using two separate linear regressions, one with the average of all 26 experiments and one with a specific experiment. The electrode outlet RH is estimated by solving (13) and (14) with measurements of electrode manifold temperature, pressure and RH. The simulations are completed using the average diffusion coefficients $d_{w_1}^{av}$ and $d_{w_0}^{av}$ from all 26 runs and the specific diffusion coefficients $d_{w_1}^{*}$ and $d_{w_0}^{*}$ from an individual run and then compared to the measured electrode outlet RH, see Figure 7, providing experimental validation of the proposed model.

Data are collected at an average rate of 2.5 Hz. The data are then linearly interpolated at a time step of 0.2 seconds (5 Hz) is used for the simulations shown.

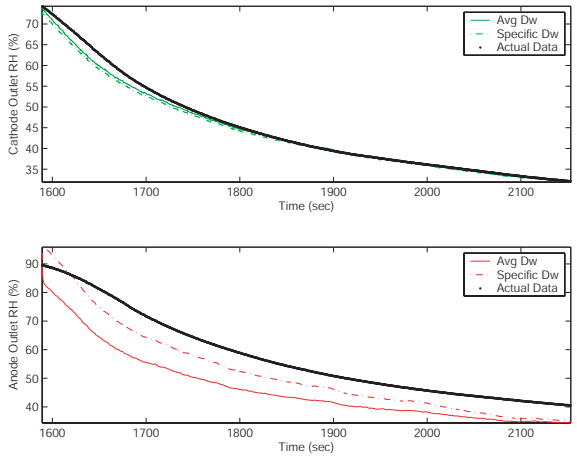

Fig. 7. Model Validation

The models predict electrode outlet RH values with maximum deviations of 4% and 3% for the cathode and 6% and 15% for the anode, using the specific and averaged $\tilde{D}_w$ coefficients respectively.

The anode RH estimation initially increases using the specific diffusion coefficients $d_{w_1}^{*}$ and $d_{w_0}^{*}$. However, the anode RH estimation initially decreases when using the average diffusion coefficients $d_{w_1}^{av}$ and $d_{w_0}^{av}$. The substantial difference between the anode estimation and the actual value is thought to be due to the sensitivity of the outlet RH prediction to $\widehat{D}_w$. A small amount of vapor enters the anode (20% RH at near ambient temperature), thus all of the vapor exiting the anode results from the diffusion of vapor from cathode to anode. A small error in calculating the $\widehat{D}_w$ results in an error in the estimation of the vapor transport across the membrane, in turn resulting in an error in predicting anode outlet RH.

VII. Concluding Remarks and Future Work

With an accurate model of the back diffusion of vapor from the cathode to the anode of a multi-cell PEMFC stack, the membrane vapor flow between the electrodes can be calculated. With this model of membrane vapor flow, experimental runs presented demonstrate the capability of a simple electrode mass balance in accurately estimating electrode exhaust RH of both the cathode and anode.

It is important to note that under load, fuel cells typically operate with multi-phase flow, both on the anode and on the cathode. As a result, quantifying the movement of water vapor inside a stack is not trivial. By incorporating electroosmotic drag and electrode flooding, this work will lead to further investigations associated with water and thermal management.

References

[1] M. Ise, K. Kreuer, and J. Maier, "Electroosmotic drag in polymer electrolyte membranes: an electrophoretic nmr study," *Solid State Ionics*, vol. 125, pp. 213–223, 1999.

[2] M. Mench, Q. Dong, and C. Wang, "In situ water distribution measurements in a polymer electrolyte fuel cell," *Journal of Power Sources*, vol. 124, pp. 90–98, 2003.

[3] S. Motupally, A. Becker, and J. Weidner, "Diffusion of water in nafion 115 membranes," *Journal of The Electrochemical Society*, vol. 147, no. 9, 2000.

[4] D. Natarajan and T. Nguyen, "Three-dimensional effects of liquid water flooding in the cathode of a pem fuel cell," *Journal of Power Sources*, vol. 115, pp. 66–80, 2002.

[5] T. Okada, S. Kjelstrup-Ratkje, S. Moller-Holst, L. Jerdal, K. Friestad, G. Xie, and R. Holmen, "Water and ion transport in the cation exchange membrane systems $nacl - srcl_2$ and $kcl - srcl_2$," *Journal of Membrane Science*, vol. 111, 1996.

[6] T. Okada, G. Xie, and M. Meeg, "Simulation for water management in membranes for polymer electrolyte fuel cells," *Electrochimica Acta*, vol. 43, no. 14-15, pp. 2141–2155, 1998.

[7] T. Springer, T. Zawodzinski, and S. Gottesfeld, "Polymer electrolyte fuel cell model," *Journal of the Electrochemical Society*, vol. 138, no. 8, 1991.

[8] T. Zawodzinski, J. Davey, J. Valerio, and S. Gottesfeld, "The water content dependence of electro-osmotic drag in proton-conducting polymer electrolytes," *Electrochimica Acta*, vol. 40, no. 3, 1995.

[9] T. Zawodzinski, C. Derouin, S. Radzinski, R. Sherman, V. Smith, T. Springer, and S. Gottesfeld, "Water uptake by and transport through nafion 117 membranes," *Journal of the Electrochemical Society*, vol. 140, no. 4, 1993.